Available online at www.sciencedirect.com
SCIENCE DIRECT®
Coordination Chemistry Reviews 248 (2004) 261–272
COORDINATION CHEMISTRY REVIEWS
www.elsevier.com/locate/ccr

Review

Excited state relaxation of Cr(III) in oxygen environments

Leslie S. Forster*

Department of Chemistry, University of Arizona, Tucson, AZ 85721, USA

Received 2 July 2003; accepted 31 October 2003

Contents

Abstract

The emission spectra and excited state decay characteristics of Cr^{3+} ions in oxide crystals and glasses and molecular complexes are reviewed. The relevant species can be described as CrO_6 and both narrow $^2E \Rightarrow {}^4A_2$ phosphorescence and broadband $^4T_2 \Rightarrow {}^4A_2$ fluorescence are observed with intensities and lifetimes that depend on the disposition of the excited levels and the temperature. A unified model that relates the emission in the several environments is described. A kinetic analysis is applied to extract individual rate constants and to determine the origin of the thermal quenching. Kinetic limits on $^2E \Rightarrow {}^4T_2$ back-transfer are explored.

Keywords: Cr(III)–oxygen complexes; Fluorescencc and phosphorescence; Decay time; Emission spectra

1. Introduction

The energy levels of Cr(III), a d^3 ion, are sensitive to environment. Within ligand field theory, the environmental effects are expressed by the magnitudes of Dq, the crystal field parameter, and *B* and *C*, the Racah parameters which are a measure of interelectronic repulsion. The energy level variation is shown in Fig. 1 where the levels are designated by the group theoretical symbols appropriate to *O* symmetry.

The ruby emission spectrum. and lifetime were measured in 1867 [1]. In the interim the spectra and excited state relaxation rates have been recorded for hundreds of Cr^{3+} in ionic crystals, ionic glasses, and molecular (Werner) complexes [2,3]. The ^2E level energy is not very sensitive to Dq, but depends on the Racah parameters. The $^4T_2$ energy varies linearly with Dq. The emission spectrum depends upon the

* Tel.: +1-520-298-2120; fax: +1-520-621-8407.
E-mail address: forsterl@u.arizona.edu (L.S. Forster).

0010-8545/$ – see front matter © 2003 Elsevier B.V. All rights reserved.
doi:10.1016/j.ccr.2003.10.014

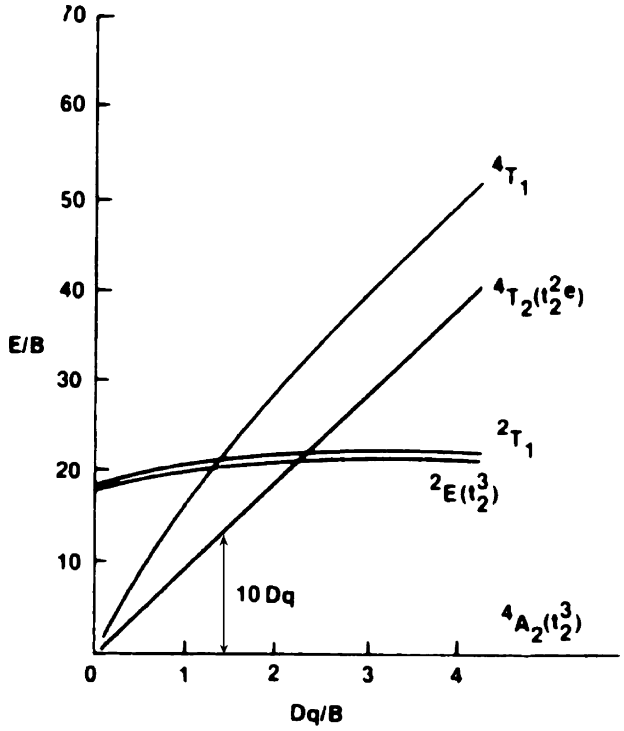

Fig. 1. Dependence of energy levels on crystal field parameters.

relative disposition of $^4T_2$ and ^2E. In most cases $^4T_2$ is above ^2E (Fig. 2) and only sharp intraconfigurational phosphorescence ($t_2^3 \Rightarrow t_2^3$, $^2E \Rightarrow {}^4A_2$) is observed. At low Cr(III) concentration the phosphorescence consists of narrow origin features, designated as R-lines, and vibronic sidebands. As Dq is reduced the level order is reversed and broad interconfigurational fluorescence ($t_2{}^2e \Rightarrow t_2^3$, $^4T_2 \Rightarrow {}^4A_2$) emission dominates at low temperatures. The difference between the spectra for $^4T_2$ and ^2E emission makes the assignment of the emitting level relatively secure. A rule of thumb that separates high-field sites where ^2E is lower from low-field sites where $^4T_2$ is below ^2E is $Dq/B \approx 2.3$ [4].

In ruby there are six nearest neighbor oxygen atoms in a nearly octahedral disposition. This species can be represented as CrO_6. Although the ruby emission is phosphorescence, the Dq associated with oxygen ligation is small enough to observe fluorescence in many CrO_6 species. It is this group that is the subject of the following review.

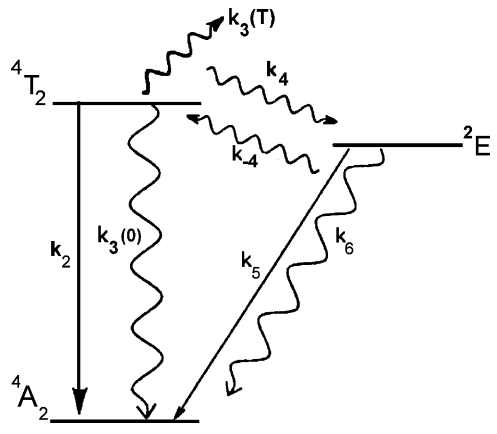

Fig. 2. Schematic energy levels and rate constants.

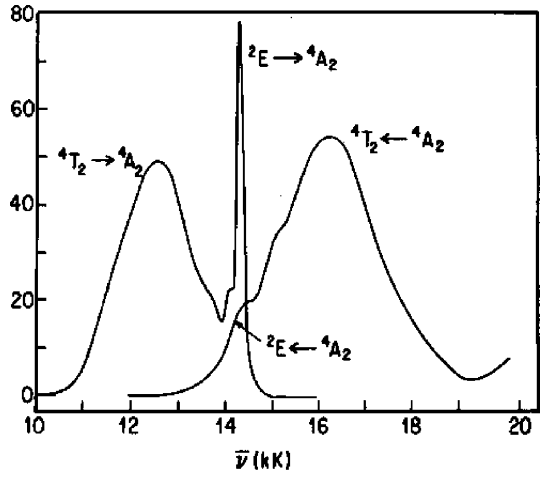

Fig. 3. Spectra of $Cr(urea)_6^{3+}$ in an alcoholic glass at 78 K (redrawn from [50]).

The small $^4T_2 - {}^2E$ gap in most CrO_6 systems permits interlevel thermal excitation at moderate temperatures (Fig. 3). Although broadband emission is common in ionic crystals and glasses there are a number of molecular complexes in which delayed fluorescence has not been detected but $^2E \Rightarrow {}^4T_2$ back-transfer has been claimed as an important process. In the absence of delayed fluorescence one must rely on indirect arguments to implicate back-transfer when ^2E is the emitting level. The location of the ^2E origin is usually directly made from absorption or emission spectra. In contrast, the $^4T_2$ origin band is often not resolved in the spectra and ΔE, the energy separation between $^4T_2$ and ^2E, is not directly measurable. Whether the failure to observe delayed fluorescence is due to efficient nonradiative depletion of $^4T_2$ or ^2E is a question to be addressed. The answer to this question bears on the problem of identifying the ^2E relaxation mechanism in the panoply of Cr(III) complexes [2].

In this review, the relaxation of Cr^{3+} excited states in ionic crystals and glasses, as well as molecular complexes will be examined with the aim of presenting a unified picture of excited state relaxation as a function of temperature. The role of environmental heterogeneity in mechanistic inferences will also be discussed.

2. Kinetics of excited state decay

The $^2T_1$ level lies some 500–700 cm^{-1} above ^2E. The $^2T_1$ and ^2E populations are often combined for kinetic purposes. When ^2E is the lowest excited level the essential features of excited state decay can be represented by the processes: $^2E \Rightarrow {}^4T_2 \Rightarrow {}^4A_2$ and $^2E \Rightarrow {}^4A_2$. If $^4T_2$ is lower, only the $^4T_2 \Rightarrow {}^4A_2$ processes need be considered. In the first

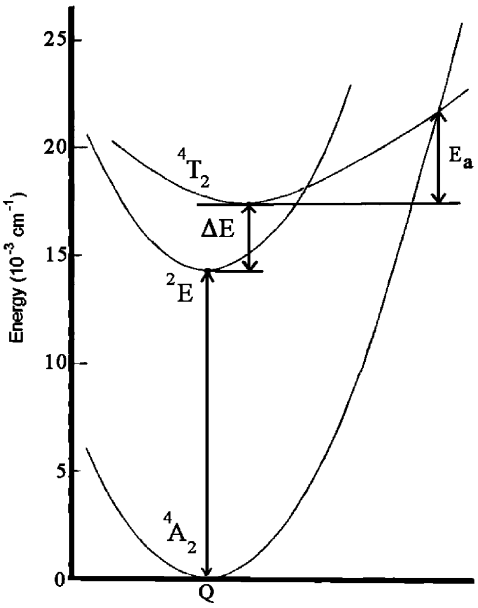

Fig. 4. Potential energies as a function of configuration coordinate, Q. Energies are applicable to ruby (from [5]).

mechanism a three-level model is assumed in which $^2E \Rightarrow {}^4T_2$ back-intersystem crossing is involved and the excited state populations are given by [3]

$$[{}^4T_2] = a_1 \exp(-\lambda_1 t) + a_2 \exp(-\lambda_2 t)$$

$$[{}^2E] = a_3 \exp(-\lambda_1 t) + a_4 \exp(-\lambda_2 t)$$

where

$$\lambda_{1,2} = 0.5[(k_T + k_E) \mp ((k_T - k_E)^2 + 4k_4k_{-4})^{0.5}] \quad (1)$$

$k_T = k_2 + k_3 + k_4$, $k_E = k_5 + k_6 + k_{-4}$. k_2 and k_5 are radiative rate constants and k_3 and k_6 the nonradiative rate constants that include chemical reaction. k_4 and k_{-4} refer to intersystem and back-intersystem crossing, respectively There are allowed and vibrationally induced components of the radiative rate constants. The vibronic parts are temperature dependent and increase as $\coth(\hbar\omega/2k_BT)$, where ω is the frequency of the promoting mode. $k_3 = k_3(0) + k(T)$ where $k_3(0)$ is due to tunneling and $k_3(T)$ is the thermally activated contribution. Both terms refer to $^4T_2 \Rightarrow {}^4A_2$ processes. E_a is the energy required to reach the crossing of the $^4T_2$ and $^4A_2$ potential surfaces (Fig. 4), but a simple Arrhenius dependence $k_3(T) = A \exp(-E_a/k_BT)$ has been questioned [5–7]. Nevertheless, E_a is an empirical measure of the energy required for the thermally activated nonradiative transition from $^4T_2$ to $^4A_2$.

Eq. (1) assumes δ-function excitation and does not require either equilibrium or steady state conditions. However, there are many parameters in Eq. (1) and fitting a decay by trial-and-error can be tedious. It has the virtue of showing the conditions required for exponential decay to be observed.

When $k_4 \gg k_2 + k_3$ and $k_{-4} \gg k_5 + k_6$ the $^4T_2$ and ^2E populations are in quasi-equilibrium and both levels decay with the same rate constant, $\lambda_1 = k_{relax}$. The decay of either fluorescence or phosphorescence is then $I(t) = I(0) \exp(-k_{relax}t)$. There will be a time interval that depends on the relative magnitudes of λ_1 and λ_2 before equilibrium is established. In transition metal complexes $\lambda_2 \gg \lambda_1$ and this pre-equilibrium time is short.

If the symmetry around the central ion is reduced, ^2E and $^4T_2$ are split. In the equilibrium limit

$$k_{relax} = \frac{k_0 + \sum k_i K_i}{1 + \sum K_i} \quad (2)$$

where $K_i = g_i\, exp(-\Delta E_i/k_BT)$ is the Boltzmann ratio for the population of the ith level to that of the lowest ^2E component. The degeneracy ratios, g_i, will be 1, 2, or 3 depending upon the energy splittings of the several thermally accessible levels. For applications when ^2E is the lowest excited state only one term in the summation is commonly used and ΔE is the energy difference between ^2E and the lowest component of $^4T_2$. In this case,

$$k_{relax} = \frac{k_5 + k_6 + (k_2 + k_3)K}{1 + K} \quad (3)$$

where $k_{-4}/k_4 = K$.

The temperature dependence of k_{relax} reflects the difference in the zero-point energies of $^4T_2$ and ^2E, ΔE, and any activation energies for $^4T_2$ depopulation, E_a.

When $^4T_2$ is below ^2E the major decay process is $^4T_2 \Rightarrow {}^4A_2$. Population of ^2E will reduce k_{relax}.

Several models have been advanced for the calculation of nonradiative rates in Cr(III) systems [5–8]. These are based on the general theory of nonradiative decay which involves separating the overall rate constant into a product of electronic and vibrational factors. The electronic factor depends on a promoting vibration while the vibrational factor involves the Frank-Condon overlap of accepting modes. Two limiting cases have been described, weak coupling (small-offset) and strong coupling (large offset). In the weak coupling limit, as exemplified by k_6 in the $^2E \Rightarrow {}^4A_2$ transition, there is little difference in the coordinates of the level minima. A single configuration coordinate is used in Fig. 4. The configuration coordinate model does not reveal all the possible relaxation pathways in multidimensional space. Weak coupling processes involve tunneling and the rate is proportional to $\exp(-E_0/\hbar\omega)$, where E_0 is the energy difference between the zero-point levels of the two states involved in the nonradiative transition and ω is the accepting mode frequency. There is little effect of temperature on tunneling rates [9], but a large deuterium isotope effect is a good marker for this limit. The strong coupling limit corresponds to an activated surface crossing. Note that E_a refers to $k_3(T)$ and it can be smaller than ΔE.

If adequate corrections for the wave length dependence of the detection system are made, the total emission intensity will be proportional to the sum of the absolute fluorescence and phosphorescence emission yields. In principle, a thermal decrease in I_{total} indicates a contribution of $k_3(0)$, but due to

calibration errors $k_3(0)$ must be a substantial fraction of k_2 before an intensity decrease will be sufficient to infer nonradiative decay [10]. A nearly constant intensity is consistent with a modest value of $k_3(0)$. Only if the absolute emission yield is unity can it be concluded that all nonradiative rates are negligible. Large intensity decreases are due to $k_3(T)$.

The three-level model is clearly oversimplified. In addition to a contribution from $^2T_1$, the splitting of $^4T_2$ could require the use of Eq. (2). However, including these additional levels does not change the overall interpretation [6].

3. Cr^{3+} in ionic crystals

There is no translational motion on the time scale of the excited state lifetime in crystals and the ions occupy positions dictated by the crystal symmetry. In some crystals all chromium ions experience the same crystal field whose magnitude is determined by the nature and distance of the surrounding ions. The emission decay is then exponential. In other systems Cr^{3+} occupies more than one nonequivalent site and the decay will be nonexponential if emission from more than one site is monitored. By choosing appropriate excitation and emission wave lengths it is sometimes possible to monitor emission from a single site.

3.1. Ruby

Ruby (Cr^{3+}:Al_2O_3) has been the subject of numerous spectroscopic and kinetic studies. Each Cr^{3+} is surrounded by a trigonally distorted (C_{3v}) octahedron of six nearest neighbor oxygen atoms. All sites are identical and $^4T_2$ is above ^2E. The $^4T_2$ splitting is 500 cm^{-1} with the $^4E(C_{3v})$ level lower [11]. The ^2E splitting is 29 $cm^{-1}$with a $^4E - {}^2E$ gap of about 2300 cm^{-1} [6]. The emission below 400 K is the narrow structured $^2E \Rightarrow {}^4A_2$ but fluorescence is evident at higher temperatures. k_6 is small at 300 K but is increased somewhat at 373 K [12]. k_5 is 235 s^{-1} at 20 K and is only slightly changed at 373 K due mainly to increasing sideband intensity. There is a small lifetime reduction below 100 K due to changing populations between the ^2E components.

The intensity ratio of the broad fluorescence to the narrow phosphorescence is

$$\frac{I_F}{I_P} = \frac{k_2}{k_5}\frac{[^4T_2]}{[^2E]} \tag{4}$$

In the equilibrium limit Eq. (4) was fitted with $[^4T_2]/[^2E] = K = 2\exp(-\Delta E/k_B T)$ and $\Delta E = 2350 - 1.4k_B T$ cm^{-1}, with, $k_2/k_5 = 164$ [6]. $g = 2$ was used in K because it was assumed that the trigonal splitting of $^4T_2$ was so large, 500 cm^{-1}, that only $^4E(C_{3v})$ was appreciably populated. The second term in ΔE was used to include the lowering of $^4T_2$ induced by thermal expansion of the crystal. Eq. (4) does not require that k_3 be constant, i.e. is valid when activated quenching of $^4T_2$ is important. However, the populations might not be in quasi-equilibrium in that event.

Equilibrium between $^4T_2$ and ^2E is established at 123 K; the $^4T_2$ population below 350 K is too small to induce quenching. The lifetime and emission intensity decreases above 350 K were attributed to increases in both k_2 and $k_3(T)$. The effect of populating $^4T_2$ without any contribution from activated surface crossing is masked by the large ΔE. $k_3(T)$ was assumed to be responsible for the quenching of I_{total} above 450 K.

The ambiguity in curve fitting to extract kinetic parameters is illustrated by a comparison of the foregoing with another study in which Eq. (3) was used without thermal reduction of ΔE [64]. A reasonable fit in the 300–570 K range was obtained with $\Delta E = 1957$ cm^{-1} and $k_2/k_3 = 230$.

3.2. Emerald

Emerald (Cr^{3+}:$Be_3Al_2(SiO_3)_6$) is another ionic system with a CrO_6 moiety. ^2E is the lowest excited level and only phosphorescence obtains at 77 K [10]. The $^4T_2 - {}^2E$ gap is small and the broad fluorescence, already intense at 195 K, dominates at 300 K. The site symmetry is D_3 and the $^4T_2$ splitting is near 100 cm^{-1} with $^4A_1$ lower [13]. The $^4T_2 - {}^2E$ gap has been estimated as ≈400 cm^{-1} [10]. The Cr^{3+} concentration was only 0.05 at.% in this work and energy transfer was probably unimportant.

In one analysis, lattice expansion was again assumed to lower $^4T_2$ and $\Delta E = 500 - 2.1k_B T$ cm^{-1} was proposed [6]. This assumption leads to $^4T_2 - {}^2E$ level inversion at 343 K. $^4T_2 - {}^2E$ equilibrium is established at 28 K. In contrast to ruby, the small ΔE leads to marked lifetime quenching below 343 K due to $^4T_2$ population (Fig. 5). This decrease is followed by a region of nearly constant lifetime. Above 450 K $k_3(T)$ becomes important. A reasonable fit up to 450 K with Eq. (3) was obtained by assuming $^4T_2 \Rightarrow {}^4A_2$ is largely radiative with $k_2 \approx 3 \times 10^4$ s^{-1}. Since $k_5 = 7 \times 10^2$ s^{-1} the ratio of the radiative rates is only 43.

The total emission yield doesn't decrease below 450 K, indicative of a small $k_3(0)$. The intensity decrease above 450 K is due to $k_3(T)$.

A fit without lattice expansion was nearly as good as the one with level inversion [6]. The parameters used were $\Delta E = 388$ cm^{-1}, $k_2 = 8.5 \times 10^4$ s^{-1}, $k_5 = 700$ s^{-1}, $A = 3 \times 10^{10}$ s^{-1}, and $E_a = 7000$ cm^{-1}. k_2/k_5 exceeds 100, a more reasonable value than 43. Whenever there are so many adjustable parameters more than one fit is likely to be satisfactory. This does not change the major conclusions that nonradiative processes are unimportant below 450 K and activated nonradiative $^4T_2 \Rightarrow {}^4A_2$ is dominant at higher temperatures.

In a later study, the impurity concentration in emerald was increased to 3 at.%. Nonequivalent sites were identified and energy transfer from the higher energy sites induced nonexponential decay [14]. It was possible to resolve the emission from different sites and the

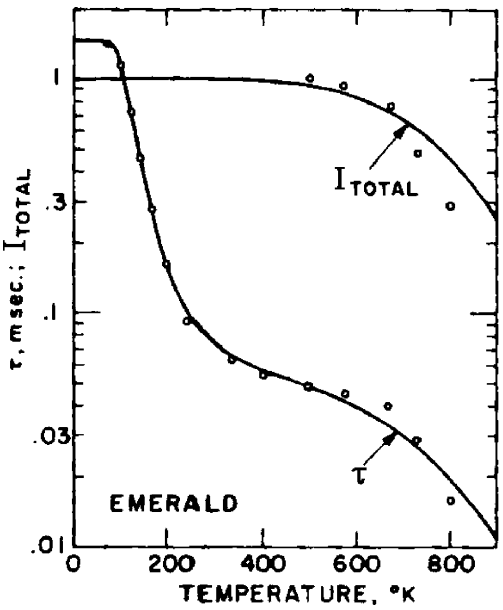

Fig. 5. Emerald lifetimes and total emission intensities (from [6]): (○) experimental results and solid curves are calculated. Below 450 K, the lifetimes were computed from Eq. (3). Above 450 K, $k_3(T)$ was calculated from theory.

emission decay from the low energy acceptor sites was exponential.

3.3. Alexandrite

Cr(III) in alexandrite (Cr^{3+}:$BeAl_2O_4$) occupies two sites of different symmetry, C_s and C_i [15]. The narrow $^2E \Rightarrow {}^4A_2$ emissions from the two sites have been monitored separately and the decay times recorded as a function of temperature. In the C_s sites the low temperature k_{relax} is $435\,s^{-1}$ increasing sharply at 130 K. Fitting k_{relax} as a function of temperature to Eq. (3) up to 300 K with $g = 1$ and $k_2 + k_3(0) = 1.4 \times 10^5\,s^{-1}$ yielded $\Delta E = 800\,cm^{-1}$, which is in accord with the spectroscopic value of $807\,cm^{-1}$ [16]. The broad fluorescence was readily discernible at room temperature.

In another study, ^2E emission from both sites was monitored and the low temperature k_{relax} was $3 \times 10^3\,s^{-1}$ [17]. A good fit of the lifetime with $g = 1$ from 300 to 973 K was obtained for a quasi-equilibrium between ^2E, $^4T_2$, and the activated species at the $^4T_2 - {}^4A_2$ crossing point. Since the concentration of the activated species is so small, this approach using Eq. (2) with two terms is equivalent to using Eq. (3) with $k_3(T)$. With this interpretation $A = 1.5 \times 10^{14}\,s^{-1}$, $E_a = 11,700\,cm^{-1}$, $\Delta E = 745\,cm^{-1}$, $k_5 = 364\,s^{-1}$, and $k_2 + k_3(0) = 3.6 \times 10^5\,s^{-1}$. The good fit below 450 K confirms that population of $^4T_2$ is the pertinent process and that above 450 K activated $T_2 \Rightarrow {}^4A_2$ is the source of the accelerated decay at high temperatures. The fit was improved when $g = 3$ was used [64]. Then $\Delta E = 857\,cm^{-1}$ from 290 to 650 K. Extending the temperature range to 930 K led to $E_a = 10{,}807\,cm^{-1}$.

The situation is quite different for Cr(III) in the C_i sites of alexandrite. At first the emission was thought to be temperature invariant [15], but in later work with a more dilute crystal the lifetime did decrease with temperature [16]. Emission reabsorption is important in alexandrite and this may be responsible for the dependence of the lifetime on concentration. The ^2E energy in the C_i sites is lower than in the C_s sites and the C_i ions could be selectively excited. The decays from the C_i ions were exponential with a 0.1 s lifetime below 100 K. The temperature dependence of the C_i k_{relax} could not be fit with Eq. (3) unless thermally enhanced k_5 was included. In that case, a good fit was possible with $\Delta E = 1430\,cm^{-1}$ and $k_2 + k_3(0) = 6.7 \times 10^2\,s^{-1}$. The small values for the decay rates are due to the inversion symmetry.

k_4 and k_{-4} for the C_s ions were determined independently as 3.7×10^{10} and $3.5 \times 10^9\,s^{-1}$, respectively, at room temperature [18]. These rates lead to an equilibrium constant of 0.095, much larger than computed for an $800\,cm^{-1}$ separation. In spite of this discrepancy, it is safe to conclude that thermalization between the emitting levels in the C_s species is achieved.

3.4. Cr^{3+}:MgO

The Cr^{3+}:MgO system is of especial interest because there is a charge mismatch between the impurity and host cations. In addition to CrO_6 in O_h sites there are tetragonal and rhombic sites produced by lattice vacancies [19,20]. $^4T_2$ is above ^2E in the cubic and tetragonal sites but the order is reversed in the rhombic sites. This leads to phosphorescence and thermally induced delayed fluorescence in the cubic and tetragonal sites and only fluorescence in the rhombic sites. In an early study emission from the different sites was not differentiated and the R-line lifetime thermal quenching was associated with $\Delta E = 834\,cm^{-1}$ [21]. It was possible to record the emission from only the cubic sites by a time-resolution technique [20]. Fitting Eq. (3) with $K = 3\exp(-\Delta E/k_B T)$ yielded $\Delta E = 1100\,cm^{-1}$, very nearly the same as the spectroscopic value for the $^4T_2 - {}^2E$ separation [20]. The 77 K lifetimes of the cubic, tetragonal, and rhombic centers are 11.6 ms, 8.6 ms, and 35 μs, respectively. k_{relax} for $^4T_2 \Rightarrow {}^4A_2$ in the rhombic sites, $3 \times 10^4\,s^{-1}$, is very close to the $1.7 \times 10^4\,s^{-1}$ value for the same process in the cubic sites, estimated from Eq. (3) by neglecting nonradiative processes.

The $^4T_2$ level in a rhombic site is $684\,cm^{-1}$ below ^2E in cubic sites and energy transfer from cubic to rhombic centers has been demonstrated at 77 K in 0.05% Cr^{3+} crystals [22]. The Cr^{3+} concentration in the earlier work was much lower and those results were not affected by energy transfer [19].

3.5. Garnets

Crystals with the garnet structure have the general formula $A_3B_2C_3O_{12}$. Many different ions can exist in the three

different cation sites. Cr^{3+} substitutes in the B site, which is octahedral with trigonal distortion and inversion symmetry. The inversion center leads to a vibronically induced radiative rate [23]. The crystal field strength varies in this group of crystals and the low temperature emission in $Y_3Ga_5O_{12}$ (YGG) is exclusively phosphorescence, while in several of the garnets with small $^4T_2 - {}^2E$ separations, $Gd_3Sc_2Ga_3O_{12}$ (GSGG) and $Gd_3Sc_2Al_3O_{12}$ (GSAG), both sharp and broadband emissions were observed [23–25]. When two or more host cations can occupy the same site in the garnets, substitutional disorder occurs [26]. This disorder is due to Cr^{3+} ions in crystallographically identical sites but which experience a range of crystal fields because the second nearest neighbor cations are randomly distributed. Nonexponential decay and lifetimes that vary with the emission wavelength are the result [25,26].

k_{relax} in Cr^{3+}:YAG, a crystal in which $^4T_2$ is above ^2E, was well fitted by Eq. (3) between, 77 and 550 K with $g = 3$ if the vibronic contribution to k_5 was included [65].

When emission from a single site was monitored in GSGG both fluorescence and phosphorescence persisted at low temperature [24]. I_F/I_P was constant below 20 K, an observation that is inconsistent with thermalization between two different levels. The emission of both the sharp and broadband spectra from the lowest energy level has been ascribed to the small energy difference between ^2E and $^4T_2$ that leads to extensive mixing by spin-orbit coupling [24–29]. This mixing leads to one level which is predominantly ^2E and another which is mainly $^4T_2$. The mixing also increases k_5. At low temperatures ^2E is lower in GSGG but the admixture of $^4T_2$ is evident in the emission leading to $I_F/I_P \approx 5$ at 10 K. If both emissions originate in the same, albeit mixed, state the lifetimes should be identical. The phosphorescence lifetime of 225 μs is matched by the 230 μs long lived tail in the nonexponential fluorescence decay [23]. The faster decay component would then be due to emission from another site. The calculated ΔE after mixing was 110 cm^{-1}. The general shape of the lifetime versus temperature plot resembles that of emerald (Fig. 5). The lifetime decrease as a result of populating the $^4T_2$ level below 200 K is followed by a plateau until 450 K and a steep drop due to the activated surface crossing process.

Cr^{3+}:$(La,Lu)_5Ga_3O_{12}$ (LLGG) is a garnet in which $^4T_2$ is 1000 cm^{-1} below ^2E and only fluorescence prevails at 4 K where the lifetime is 90 μs. [26] Since the lifetime is only reduced to 68 μs at 300 K, $k_3 < 10^4\ s^{-1}$ at room temperature.

3.6. Miscellaneous hosts

There are two nonequivalent sites in Cr^{3+}:gallogermanates [30]. Substitutional disorder in each site results from interchangeability of gallium and germanium ions. In the high Dq sites the R-line emission predominates, while the emission from the low-field sites is mainly fluorescence. The 14 K phosphorescence decay was nonexponential. The phosphorescence lifetime was assumed to be radiative with k_5 in each site determined by spin-orbit coupling and therefore to the $^4T_2 - {}^2E$ gap. Since this gap varies among the sites the R-line emission decay was nonexponential. In contrast, the fluorescence decay was exponential at 14 K. Since the $^4T_2 \Rightarrow {}^4A_2$ transition is radiative and spin-allowed, the $^4T_2 - {}^2E$ gap is not important because spin-orbit mixing does not affect k_2 very much. The substitutional disorder increases $k_3(T)$ due to large distortions from octahedral symmetry and shape changes in the potential surfaces that reduce E_a [31,32].

Another example where $^4T_2$ is lower and the effect of temperature on k_3 has been studied is Cr^{3+}:$LiTaO_3$. In this crystal k_3 is either small or constant up to 150 K. [33]. It is thermally activated at higher temperatures and exhibits good Arrhenius behavior with $A = 4.3 \times 10^{12}\ s^{-1}$ and $E_a = 2960\ cm^{-1}$. The fluorescence lifetime at 5 K is 8 μs and 400 ns at room temperature [34]. Consequently, k_3 is about $2 \times 10^6\ s^{-1}$ at ambient temperature. The Arrhenius parameters refer directly to the activated nonradiative transition to the ground state without including the effect of populating the ^2E level, which would increase the lifetime. The emission intensity is strongly quenched below 300 K [35].

The decay rates in Cr^{3+}:$ScBO_3$, a low field complex, cannot be fitted to a single thermal decay process [36]. Instead there is an increase in k_{relax} from $5 \times 10^3\ s^{-1}$ at low temperature to $10^4\ s^{-1}$ at 300 K, accompanied by fluorescence yields near unity, indicating thermally enhanced k_2. This is followed by a marked k_{relax} increase at higher temperatures with an activation energy of about 4000 cm^{-1}.

Other low-field ionic systems are perovskites [37] and alkaline earth fluorides [38]. In the perovskites, where CrF_6 is the emitting moiety, there are again two processes. The emission quantum yield is near unity at room temperature. The small lifetime decrease below 300 K was attributed to increasing k_2 by the population of a higher $^4T_2$ component. Above this temperature, the activated process has $E_a = 7300$ and 9200 cm^{-1} for Cr^{3+}:K_2NaScF_6 and Cr^{3+}:K_2NaGaF_6, respectively [37]. The A values are approximately $10^{13}\ s^{-1}$.

The parameters for the low-field crystals are included in Table 1. In only a few cases are the absolute emission quantum yields known and the relative contributions of k_2 and $k_3(0)$ to k_{relax} are uncertain. It can be said, however, that $k_3(0)$ does not exceed $\sim 10^5\ s^{-1}$ in the low temperature limit. Only at high enough temperatures for $k_3(T)$ to contribute can we be sure that nonradiative relaxation is important. This contribution is signaled by a reduction in the emission intensity.

3.7. Summary of ionic crystal results

The major results of Cr^{3+} relaxation studies in ionic crystals are: (1) when ^2E is the lowest excited level the thermal quenching pathway involves population of a $^4T_2$ component. $k_2 + k_3(0)$ can only be determined indirectly; (2) $^4T_2$ and ^2E are in equilibrium and thermally induced fluorescence is

Table 1
Kinetic parameters for CrO_6 systems

Ionic crystals	$k_2 + k_3(0)$ (s^{-1})	ΔE (cm^{-1})	A (s^{-1})	E_a (cm^{-1})	Reference
^2E lower					
Ruby	2.3×10^4	2350			6
Emerald	3×10^4	400	3×10^{10}	7000	6
Alexandrite (C_s)	1.4×10^5	800			15
Alexandrite (C_i)	6.7×10^2	1430			
MgO (cubic)	1.7×10^4	1100			20
Garnet (YAG)	3.3×10^4	1161			65
$^4T_2$ lower					
Garnet (LLGG)	1.1×10^4	−1000			26
$Al(PO_3)_3$	6×10^3				39
$ScBO_3$	4.9×10^3		1.8×10^9	4000	36
$LiTaO_3$	1.3×10^5		4.3×10^{12}	2960	33, 34
MgO (rhombic)	2.9×10^4				20
Molecular complexes					
$Cr(urea)_6(ClO_4)_3$	$>10^7$	90			40
Cr^{3+}:$NaMgAl(ox)_3 \cdot 9H_2O$	3.5×10^8	1050			41
Cr^{3+}:$Al(acac)_3$	5×10^{13}		10^{14}	3320	42
Cr^{3+}:$AlCl_3 \cdot 6D_2O$	2×10^6	540			41

observed at temperatures where the phosphorescence lifetime is markedly reduced. $k_2 + k_3(0) \leq 10^5\,s^{-1}$ (Table 1) and k_2 varies from 10^2 to $10^5\,s^{-1}$, depending on the site symmetry; (4) at high temperatures an activated $^4T_2 \Rightarrow {}^4A_2$ crossing contributes to k_3 and dominates k_{relax}; (5) some systems with oxygen coordination exhibit both broadband fluorescence and narrow phosphorescence at low temperatures. This dual emission occurs when $^4T_2$ and ^2E are nearly equienergetic and mixing between the two states becomes substantial; (6) when $^4T_2$ is lowest large lifetime quenching is mainly due to activated $^4T_2 \Rightarrow {}^4A_2$ surface crossing.

4. Cr^{3+} in ionic glasses

As in ionic crystals there is little translational motion involving the neighbors of the Cr^{3+} ions during the excited state lifetime. The essential feature of a glass is disorder. Instead of the small number of sites encountered in crystals with substitutional disorder, a near continuum of sites is present in an ionic glass. Furthermore, the composition of glasses is variable. For example, silicate glasses are the most common, but modifiers and stabilizers can be added in varying amounts and comparisons between the results of different authors are often uncertain.

Although in a glass there is no long range order the luminescent species in ionic glasses can still be described as CrX_6. In oxide glasses X is oxygen while in fluoride glasses fluorine is coordinated. The average distance between the Cr^{3+} and the nearest neighbors ions is larger than in most ionic crystals due to the looser structure of the glass [43]. This loose structure gives rise to voids or defects that lead to reduction of the $^4T_2$ energy and to a larger shift of the potential minimum. The result is a displacement of the absorption and emission spectra to longer wave lengths and to a larger Stokes shift than in crystals. This effect is shown by the emission spectra of Cr^{3+} in crystalline and glassy $Al(PO_3)_3$ hosts [39].

The $^4T_2 - {}^2E$ energy difference and ordering is related to the crystal field at each site. In most glassy hosts, the preponderance of emission at room temperature is fluorescence and the emission at low temperatures is either exclusively broadband fluorescence or a mixture of fluorescence and phosphorescence. The simultaneous emission of broadband and sharp luminescence has two possible origins. Since there is a distribution of sites with different Dq values, some of the sites may be high-field in which $^2E \Rightarrow {}^4A_2$ obtains, while other sites are low-field and $^4T_2 \Rightarrow {}^4A_2$ occurs. This is the situation in borate glasses where energy transfer from the higher energy ^2E species to $^4T_2$ levels in ions in low-field sites has been established [44]. Alternatively, the nearly equienergetic $^4T_2$ and ^2E states can mix, leading to simultaneous fluorescence and phosphorescence from the same level at low temperatures. The lowest level is predominantly $^4T_2$. The different sites vary in the amount of mixing and decay times. This leads to lack of decay time identity of the broadband and sharp emissions. In a silicate glass, the 13 K lifetimes are not the same even though state mixing is assumed to be important [4].

The distribution of sites has several consequences. The emission spectrum shifts to lower energies and I_F/I_P increases as the excitation wave length within the $^4T_2 \Leftarrow {}^4A_2$ band increases. This means that the lower field sites are preferentially excited at longer wave lengths. The most striking contrast between glassy and crystalline environments is the relatively small fluorescence yields in the glasses at room temperature [43–45]. The low-field sites also have the smallest emission yield and are preferentially thermally quenched. This has been associated with the loose structure [43] Since the longer wave length portion of the fluorescence emission

is preferentially quenched, there is a blue shift of the broadband emission with temperature. In a borate glass the fluorescence yield is reduced from 25% at low temperatures to 1% at room temperature [44]. Lowered symmetry increases $k_3(0)$ and the emission yields are small [45].

Since site heterogeneity leads to nonexponential decay no single lifetime can be extracted. Instead, an average lifetime was defined as $< \tau >= \int tI(t)\,dt / \int I(t)\,dt$ [45]. This expression tends to emphasize the decays at longer times and minimizes the influence of the faster decays. Average lifetimes for a number of glasses at room temperature varied from 5 to 37 μs. $\langle\tau\rangle$ decreases with both excitation and emission wave lengths. This leads to a blueshift with delay in time resolved spectra [46]. Another average is defined by $\tau_{av} = \int I(t)\,dt / I(0)$. This definition weights the decay at early times heavily. This may explain the large k_3 in a phosphate glass [47].

The multiplicity of sites, of necessity, requires some assumptions to be made in order to develop an explanatory model [48]. In one model, the fluorescence decay in an aluminosilicate glass of unspecified composition was fitted to $I(t) = \sum a_i \exp(-t/\tau_i)$ with ten fixed lifetimes in each decade, spaced logarithmically. The τ distributions were nearly symmetrical when plotted on a logarithmic time base, which supports the adequacy of the model. The broad distributions were displayed as a function of excitation and emission wavelengths and temperature [48]. The most probable values of τ can then be obtained. This value at 10 K varied from 45 μs at 800 nm to 37 μs at 850 nm. There is little change up to 100 K, but the lifetimes at the maxima of the distributions were reduced markedly at 300 K. E_a = 2600–2800 cm^{-1} and $A = 10^{11}\ s^{-1}$ for this system, but there is no reason that an Arrhenius dependence should be valid when the decays are nonexponential. The activated nonradiative rate is important at much lower temperatures in the glass than in crystals. The distributions were broad, encompassing lifetimes from 10 to 100 μs and $k_2 + k_3(0)$ varies from site to site. k_2 is sensitive to the site symmetry and it is not clear if $k_3(0)$ is significant. A negligible k_3 was assumed below 100 K in the aluminosilicate glass [48]. However, the emission yields in silicate glasses are only 0.3 at low temperatures, indicative of significant $k_3(0)$ [49].

More evidence for nonradiative relaxation in a variety of glasses lies in absolute quantum yields of emission [43]. These yields ranged from 1 to 17% at room temperature. The upper limit for $k_3(0)$ is close to $10^5\ s^{-1}$.

In summary, compared to ionic crystalline hosts, solutions of Cr^{3+} in ionic glasses are associated with lowering of the $^4T_2$ energy due to reduction of the crystal field strength. As a result $^4T_2$ is either below ^2E or proximate to the latter level. The glassy environment leads to a near continuum of environments with the result that the emission decays are nonexponential. Glassy solutions exhibit emission quantum yields that are small. Emission quenching via activated surface crossing to the ground state is significant at 300 K, indicating a small E_a compared to crystalline systems.

5. Molecular complexes

In one of the first reports of emission from Werner complexes of Cr(III) both phosphorescence and fluorescence were observed from $Cr(urea)_6^{3+}$ in a rigid glass solution at 78 K [50] (Fig. 2). Schläfer predicted that only phosphorescence would be emitted when $^4T_2$ was not thermally accessible from the lower ^2E level [51]. He advanced a spectral criterion for predicting which of the three possible luminescence spectra would obtain at 88 K, phosphorescence only, fluorescence and phosphorescence, or fluorescence only. This criterion was based on the energy difference between the absorption maximum of the $^4T_2 \Leftarrow {}^4A_2$ transition and the $^2E \Rightarrow {}^4T_2$ origin. When this difference was in the range 1700–2400 cm^{-1} both sharp and broadband emission was predicted. Schläfer's rule is equivalent to $Dq/B = 2.3$ for many complexes. The relative disposition of ^2E and $^4T_2$ depends upon the nature of the coordinated ligands. In most Werner complexes of Cr(III) only phosphorescence occurs, but the Dq of oxygen is low and some complexes with the CrO_6 framework exhibit delayed fluorescence.

If population of $^4T_2$ is in the pathway for the decrease in the ^2E lifetime, thermally induced fluorescence should be detectible. From a kinetic viewpoint the absence of fluorescence can be understood by reference to Eq. (4). Since the fluorescence is broad it will always be more difficult to detect than the phosphorescence. A reasonable lower limit is the total fluorescence and phosphorescence intensities should be nearly equal. In the equilibrium limit this requires $K \approx 0.01$. k_3 plays a pivotal role in detecting fluorescence. If k_3 is large the lifetime will be short at temperatures where $K = 0.01$ and the emission intensities would be small under steady illumination. To see delayed fluorescence with pulsed excitation, short times need to be employed. Delayed fluorescence was detected in the nanosecond domain in aqueous solutions of several complexes [52].

The simplified model for thermal quenching that proved adequate for most ionic crystals involves thermally activated contributions to k_3 and equilibrium between $^4T_2$ and ^2E. The suitability of this simple model will be examined for the individual molecular complexes. In all of the CrO_6 complexes $^4T_2$ is above ^2E. Two possibilities will be explored: (1) k_3 is constant and large with thermal quenching due solely to population of $^4T_2$ and (2) k_6 is thermally activated. The former case is the back-transfer mechanism for ^2E decay while the latter involves only processes originating in ^2E With few exceptions, as described below, the $^2E \Rightarrow {}^4A_2$ emission decays of Cr(III) molecular complexes in glasses are exponential at 77 K showing that environmental heterogeneity does not affect $k_5 + k_6$ in these molecules.

5.1. $Cr(urea)_6^{3+}$

This complex exhibits both fluorescence and phosphorescence. In pure crystals ΔE varies with the anion from 130 to 500 cm^{-1} [53] and the fluorescence disappears at 1.3 K

[40]. In some lattices, $[Cr(urea)_6](ClO_4)_3$ and $[Cr(urea)_3]I_3$, the decays are exponential, while in others it is nonexponential [54]. The nonexponentiality was ascribed to multiple sites. The exponential decay in the perchlorate and iodide salts might be due to identical sites for all complexes, but energy transfer may play a role as well. There is evidence for energy transfer in $Cr(urea)_6I_3$ from the majority sites to the emissive minority sites that was associated with risetimes of 2–30 μs at different emission wavelengths at 5 K [55]. At 77 K, the decays of the ClO_4^- and I^- salts exhibited no risetime at the 1 ns level [54]. There was, however, a risetime in the Cl^- salt. The possibility of multiple sites requires caution in assigning ^2E splittings.

A fit of the relative fluorescence and phosphorescence intensities in $Cr(urea)_6(ClO_4)_3$ to Eq. (4) yielded $\Delta E = 90\,cm^{-1}$ [40], somewhat smaller than the $130\,cm^{-1}$ value obtained with Eq. (3) assuming $g = 1$ [53]. The lifetimes are not well fitted by Eq. (3) over the temperature range 5–77 K. This is not surprising since the ^2E splittings are not small compared to ΔE and the model represented by Eq. (3) is incomplete. In any event ΔE is small. The absence of dual emission due to $^4T_2 - {}^2E$ mixing is noteworthy. The thermal quenching of the lifetime at 77 K in the crystal requires $k_3 > 10^7\,s^{-1}$.

In an alcoholic glass, both the fluorescence and phosphorescence intensities decreased with temperature but the fluorescence yield was less thermally quenched than the phosphorescence yield, as expected in the equilibrium limit [56]. The fluorescence and phosphorescence decays were both nonexponential in rigid solvents with different lifetimes in the sharp and broad bands [54]. The nonexponentiality is reasonable since ΔE is so small that back-transfer is important at 77 K and environmental heterogeneity will lead to a distribution of ΔE values. As expected, when the solvent becomes fluid exponentially prevailed with identical lifetimes at all monitoring wave lengths. The 25 ns lifetime at 180 K [54] in the fluid demonstrates that k_3 is not very different in the fluid and crystalline environments and that activated surface crossing plays no role in the excited state relaxation.

The threefold difference in ΔE between the iodide and perchlorate salts leads to a 200-fold difference in $[^4T_2]/[^2E]$. This compares favorably with I_F/I_P at 77 K for the two salts where the measured ratio is 350 [57]. This indicates that k_2/k_5 is nearly invariant to the anion, at least in these two salts. The decay time in water at 295 K was 0.7 ns [52]. There was a negligible activation energy for k_{relax} near ambient temperatures.

5.2. Chromium oxalates

No fluorescence was observed in Cr^{3+}:$NaMgAl(ox)_3 \cdot 9H_2O$ (ox = oxalate) at temperatures where there was substantial quenching of phosphorescence. The absorption and emission spectra suggest that the $^4T_2 - {}^2E$ gap is small in $Cr(ox)_3{}^{3-}$ and thermal relaxation via $^4T_2$ has been proposed [58]. The decays in the mixed crystal were exponential at all temperatures. The low temperature limiting lifetime of 900 μs was reduced to 45 μs at 140 K [41]. The decay rates were fitted to Eq. (3) with $k_2 + k_3 = 3.5 \times 10^8\,s^{-1}$, $k_5 + k_6 = 1120\,s^{-1}$, and $\Delta E = 1050\,cm^{-1}$. With these constants, k_4 was varied in Eq. (1). and a good fit to k_{relax} was obtained from 77 to 140 K as long as k_4 exceeded $10^{11}\,s^{-1}$. These values lead to $[^4T_2]/[^2E] = K$. In order for equality of the fluorescence and phosphorescence yields to obtain with this parameter set, assuming $k_2/k_5 = 100$, $T > 265$ K must be achieved and the lifetime would be submicrosecond at this temperature. At room temperature $\tau = 1.2$ ns in water and weak delayed fluorescence was detected [52].

In contrast to $Cr(ox)_3{}^{3-}$ in a dilute crystalline host, the decay in propanediol was nonexponential at 77 K [58]. The nonexponentiality is confined to the first 500 μs of the decay. There is a very exponential tail with $\tau = 610$ μs. The nonexponentiality alone does not identify the thermal decay pathway since environmental heterogeneity could affect either $k_5 + k_6$ or ΔE. It was suggested that back-transfer was responsible for the nonexponentiality since the environmental heterogeneity in the glass leads to a distribution of ΔE values [58]. The gallogermanate results indicate that k_5 is sensitive to the $^4T_2 - {}^2E$ gap. Since $k_5 > k_6$ at 77 K, site variation of k_5 could also lead to the observed behavior. Support for back-intersystem crossing to $^4T_2$ comes from the decays of $Cr(ox)_2(en)^-$ (en = ethylenediamine) and $Cr(ox)(en)_2{}^+$ in propanediol and glycerol. In both complexes, the decays were exponential at 77 K with lifetimes near 80 μs, but nonexponential at higher temperatures. The ^2E energy is not very different in the three $Cr(ox)_{3-n}(en)_n{}^{2n-3}$ complexes but the $^4T_2$ energy increases with the number of en ligands. The progressive increase in the $^4T_2 - {}^2E$ gap is reflected in the higher temperature required to observe nonexponentiality. In the $n = 1, 2$ complexes $k_5 < k_6$. If the relaxation pathway was a thermally enhanced k_6 changing the $^4T_2$ energy should not affect the temperature dependence of k_6. The strongest argument for back-transfer in $Cr(ox)_3{}^{3-}$ comes from the analysis of the thermal lifetime variation in the dilute crystal.

5.3. Chromium acetylacetonate

The ^2E energy in $Cr(acac)_3$ is reduced substantially by delocalization onto the ligands [59]. This leads to a spectroscopic value of around $4000\,cm^{-1}$ for the $^4T_2 - {}^2E$ gap in a alcohol–hydrocarbon glass (EPA) at 85 K. The decays were exponential in dilute Cr^{3+}:$Al(acac)_3$ and k_{relax} depends upon two thermally activated processes [42]

$$k_{relax} = k_0 + A_1 \exp\left(\frac{-E_1}{k_B T}\right) + A_2 \exp\left(\frac{-E_2}{k_B T}\right) \quad (5)$$

where k_0 corresponds to $k_5 + k_6(0) = 1810\,s^{-1}$. Refitting the mixed crystal relaxation rates yielded $E_1 = 589\,cm^{-1}$ and $A_1 = 5.93 \times 10^4\,s^{-1}$. These parameters could correspond to the thermally activated rate ($k_6(T)$) for $^2E \Rightarrow {}^4A_2$. A fit to Eq. (5) then yielded $E_2 = 3326\,cm^{-1}$ and

$A_2 = 1.1 \times 10^{15}\,s^{-1}$. The second parameter set indicates a strongly coupled surface crossing process, most likely $^2E \Rightarrow {}^4T_2$. If $k_5 + k_6$ is calculated from E_1 and A_1 and $k_{-4} = A_2 \exp(-E_2/k_BT)$, Eq. (1) provides a good fit up to 220 K when k_3 has a constant value of $5 \times 10^{13}\,s^{-1}$. While some variation in these parameters will lead to a reasonable fit, it is clear that $k_2 + k_3$ must be very large and ^2E is not in quasi-equilibrium with $^4T_2$. Consequently, $[^4T_2]/[^2E] < K$ and high temperatures would be required for appreciable $^4T_2$ population. A large $^4T_2 \Rightarrow {}^4A_2$ rate would result if E_a were small.

E_2 appears to be smaller than the spectroscopic estimate of the $^4T_2 - {}^2E$ gap. In the absence of a resolved 0–0-feature in the $^4T_2$ absorption spectrum of the crystal ΔE might not be larger than E_2. Another possibility is a second activated crossing between ^2E and $^4A_2$. The potential curves for ^2E and $^4A_2$ are nested and the activation energy is rather small for this pathway. It has been suggested that activation energies above 3300 cm^{-1} are not compatible with back intersystem crossing [52]. Since $^4T_2 - {}^2E$ equilibrium is not achieved, the population ratios in Eq. (4) will be smaller than K and fluorescence will be very weak.

The decays in glycerol, propanediol, and 2-methyltetrahydrofuran were exponential at 77 K with lifetimes of 400–575 μs. The influence of environmental heterogeneity on the decay that was described in connection with the oxalate emission in glasses is also found in $Cr(acac)_3$. The nonexponentiality of the decays was evident at 148 K in glycerol, propanediol, and ethylene glycol–water glasses [58] Thermal quenching begins when solvent motion is slow compared to the ^2E decay rate and the intensity decays became nonexponential in this regime. This behavior parallels that of $Cr(ox)_2(en)^-$ and is attributed to a distribution of $^4T_2 - {}^2E$ gaps in rigid media. The totality of results point to back-transfer in the thermal quenching pathway.

5.4. $Cr(D_2O)_6{}^{3+}$, $Cr(H_2O)_6{}^{3+}$, and the aquoammines

$Cr(D_2O)_6^{3+}$ is unique, the lifetime in Cr^{3+}:$KAl(SO_4)_2 \cdot 12D_2O$ at 4 K is 750 μs and there is no evidence for a plateau in this value at low temperatures [60]. There was a hint of a plateau at 77 K with $AlCl_3 \cdot 6D_2O$ as the host [41]. The low temperature limiting lifetime in this crystal is greater than 325 μs and is reached slightly below 77 K. The lifetime is reduced markedly at 125 K. That k_6 is large in the protiated analogs is demonstrated by the marked intensity increase upon deuteration, the signature of weakly coupled nonradiative processes. The fluorescence and phosphorescence spectra overlap, but the intensity of the weak unstructured long wave length tail grows with temperature while the sharp phosphorescence intensity decreases, characteristic of thermally populated $^4T_2$. Similar behavior is observed in Cr^{3+}:$C(NH_2)_3Al(SO_4)_2 \cdot 6D_2O$ where $Cr(D_2O)_6{}^{3+}$ emits. However, in this crystal there are multiple sites leading to nonexponential decays, in contrast to Cr^{3+}:$AlCl_3 \cdot 6D_2O$. There was no sign of fluorescence in the emission spectra of either crystal at 4 K [61]. Fitting the Cr^{3+}:$AlCl_3 \cdot 6D_2O$ results in [41] to Eq. (4) yielded $\Delta E = 540\,cm^{-1}$. A reasonable fit of the ^2E lifetime with Eq. (1), in turn, leads to $k_3 = 2 \times 10^6\,s^{-1}$.

As the $^4T_2 - {}^2E$ gap decreases with n in $Cr(NH_3)_{6-n}(H_2O)_n{}^{3+}$ complexes the thermal decay characteristics change [62]. When n = 4–6 the low temperature decays in an alcohol-water solvent were nonexponential, although the effect was marginal when $n = 4$. The low temperature decays in both *cis*- and *trans*-$Cr(NH_3)_4(H_2O)_2{}^{3+}$ were exponential, but at higher temperatures in a rigid solvent the emission from the *trans* isomer became nonexponential while that from the *cis* species did not. This is consistent with population of a $^4T_2$ component since the splitting in the *trans* isomer is larger as evidenced by the absorption spectra, and the $^4T_2 - {}^2E$ gap is smaller. A similar pattern is observed in the *fac* and *mer* pair when $n = 3$. Keeping in mind the possibility of artifactual nonexponentiality, the totality of results in the aquoammines point to back-transfer as an important ^2E relaxation mechanism.

6. Discussion and conclusions

A unified picture of excited state decay of Cr^{3+} in ionic crystals and glasses and molecular complexes can be formulated for the CrO_6 moiety. The emission spectral behavior depends on the relative disposition of the $^4T_2$ and ^2E levels. Either level can be lower in ionic crystalline hosts, but $^4T_2$ is usually lower in oxide glasses. ^2E is lower in molecular complexes and only narrow phosphorescence is observed at low temperatures in these complexes.

In ionic systems with $^4T_2$ above ^2E the appearance of thermally induced broadband emission is correlated with the decrease in ^2E lifetime. This is unambiguous evidence for ^2E relaxation through back-transfer. A kinetic analysis can be made for a three-level system involving components of the ground level, $^4A_2$, and two excited levels, $^4T_2$ and ^2E. In the ionic crystals described, most of the thermal quenching is centered in $^4T_2$. At low temperatures the tunneling contribution, $k_3(0)$, is operative while activated surface crossing, $^4T_2 \Rightarrow {}^4A_2$, becomes important at higher temperatures. $[^4T_2]/[^2E\}$ is close to the Boltzmann ratio in ionic crystals and $k_2 + k_3(0)$ does not exceed $1.4 \times 10^5\,s^{-1}$. The lifetimes in ionic crystals where $^4T_2$ is below ^2E confirms the upper limit for $k_2 + k_3(0)$.

Of the four molecular complexes examined here, two ($Cr(urea)_6{}^{3+}$ and $Cr(D_2O)_6{}^{3+}$) exhibit delayed fluorescence accompanying ^2E quenching, $k_3(0)$ is greater in molecular complexes than in ionic crystals, but when ΔE is small appreciable $^4T_2$ population is achieved before the lifetime is too short. Calculations indicate that the larger ΔE in $Cr(ox)_3{}^{3-}$ would require $T = 300$ K to populate $^4T_2$ sufficiently to observe fluorescence The large $k_3(0)$ would then lead to a submicrosecond lifetime. The interpretation of the

$Cr(acac)_3$ results is more uncertain. ΔE exceeds 3000 cm^{-1} in this complex and quasi-equilibrium does not obtain. Consequently, the $^4T_2$ population will be small and fluorescence would be minimal. The possibility that ΔE is too large to permit back-transfer has not been eliminated.

In both ionic crystals and glasses, high enough temperatures were reached to see the effect of $k_3(T)$. This was not the case in the molecular complexes.

k_5 is a radiative rate for a spin-forbidden transition and is sensitive to spin-orbit coupling with $^4T_2$. Its magnitude is less than 10^3 s^{-1}. k_2 is increased by departures from centrosymmetry and ranges from 10^2 to 10^5 s^{-1}.

A major question is the source of the $k_3(0)$ difference in the different classes. The deuterium isotope effect in the $Cr(H_2O)_6^{3+}$ k_6 results from the change of the high frequency water stretching vibrations [8]. There is no correlation between the energy of the high frequency vibrational modes and the magnitude of $k_3(0)$ in the molecular complexes. The enhanced $k_3(0)$ in glasses was attributed to a looser structure, yet the stronger Cr(III)–ligand interaction in the molecular complexes also leads to an increase in $k_3(0)$. Except for $Cr(acac)_3$ there is no evidence for d electron delocalization onto the ligands. This problem deserves more attention.

When the molecular complexes are present in pure or dilute crystals with a single site the ^2E decays are exponential at all temperatures. Except for $Cr(acac)_3$, these complexes exhibit nonexponential decays at 77 K in glassy solution. Site to site environmental heterogeneity leads to a distribution of ΔE values and is a source of nonexponential decay when ΔE is small. In that event, the variation in ΔE not only affects the back-transfer rate, k_{-4}, it could also alter $k_5 + k_6$ through spin-orbit coupling of ^2E with $^4T_2$. The absence of dual emission in $Cr(urea)_6(ClO_4)_3$ at low temperatures is evidence against such mixing when ΔE is only 100 cm^{-1}. In most molecular complexes, ΔE exceeds 2000 cm^{-1} and the 77 K decays are exponential. Thus, $k_5 + k_6$ is insensitive to environment when molecular complexes are embedded in noncrystalline media.

The $^4T_2 - {}^2E$ gaps encountered in the CrO_6 systems are relatively small. It has been demonstrated that back-transfer does not occur in $Cr(CN)_6^{3-}$, a large gap complex. In small gap CrO_6 complexes ^2E relaxation in molecular complexes is consistent with back-transfer to $^4T_2$, followed by a transition to $^4A_2$. When $k_4 \gg k_3$ there is quasi-equilibrium between $^4T_2$ and ^2E. As the gap increases this limit no longer applies, but back-transfer is still a possible thermal quenching process even if delayed fluorescence is not observed. Can this model explain the thermal relaxation in larger gap complexes? The $Cr(acac)_3$ results are ambiguous. If the foregoing model applies, the very large $k_3(0)$ is noteworthy.

Much of the controversy about the ^2E decay pathway has centered on CrN_6 complexes [63]. The kinetic analysis places limits on back-transfer as a possible step in the relaxation mechanism. The low temperature lifetime in $Cr(en)_3^{3+}$, 120 μs, is reduced to 1.2 μs at 298 K with ΔE. 4000 cm^{-1}. Using Eq. (1), this quenching requires k_3 and k_4 to be roughly 10^{13} s^{-1}. Theoretical estimates of k_3 have been uncertain because the electronic factor is difficult to determine, but these magnitudes are not unreasonable. An unambiguous way to settle this question is to look for delayed fluorescence at very short times but achieving a large enough $^4T_2$ population in large gap complexes will be very difficult. Delayed fluorescence was detected in the nanosecond domain at room temperature in aqueous solutions of $Cr(NCS)_6^{3-}$ and $Cr(NH_3)_2(NCS)_4^-$ [52].

References

[1] E. Becquerel, La Lumière, ses causes et ses effects, Paris, Fermin-Didot, 1867.
[2] L.S. Forster, Coord. Chem. Rev. 227 (2002) 59.
[3] L.S. Forster, Chem. Rev. 90 (1990) 331.
[4] M. Yamaga, B. Henderson, K.P. O'Donnell, Y. Gao, Phys. Rev. B44 (1991) 4853.
[5] C.W. Struck, W.H. Fonger, J. Lumin. 10 (1975) 1.
[6] W.H. Fonger, C.W. Struck, Phys. Rev. B11 (1975) 3251.
[7] R.H. Bartram, J.C. Charpie, L.J. Andrews, A. Lempicki, Phys. Rev B34 (1986) 2741.
[8] R. Englman, Nonradiative Decay of Ions and Molecules in Solids, North Holland, Amsterdam, 1979.
[9] S.H. Lin, J. Chem. Phys. 56 (1972) 2648.
[10] P. Kisliuk, C.A. Moore, Phys. Rev. 160 (1967) 307.
[11] D.S. McClure, Solid State Phys. 9 (1959) 399.
[12] D.F. Nelson, M.D. Sturge, Phys. Rev. A137 (1965) 1117.
[13] D.L. Wood, J. Chem. Phys. 42 (1965) 3404.
[14] G.J. Quarles, A. Suchocki, R.C. Powell, S. Lai, Phys. Rev. B38 (1988) 9998.
[15] R.C. Powell, L. Xi, X. Gang, G.J. Quarles, J.C. Walling, Phys. Rev. B32 (1985) 2788.
[16] A.H. Suchocki, G.P. Gillilane, R.C. Powell, J.M. Bowery, J.C. Walling, J. Lumin. 37 (1987) 29.
[17] Z. Zhang, K.T.U. Grattan, A.W. Palmer, J. Appl. Phys. 73 (1993) 3493.
[18] S.K. Gayen, W.B. Wang, V. Petričevic, R.R. Alfano, Appl. Phys. 49 (1986) 437.
[19] F. Castelli, L.S. Forster, Phys. Rev. B11 (1975) 920.
[20] M.O. Henry, J.P. Larkin, G.F. Imbusch, Phys. Rev. B13 (1976) 1893.
[21] B. DiBartolo, R.C. Powell, Nuovo Cimento B66 (1970) 21.
[22] B.D. MacCraith, T.J. Glynn, G.F. Imbusch, C. McDonagh, J. Phys. C: Solid State Phys. 13 (1980) 4211.
[23] S.M. Healy, C.J. Donnelly, M.J. Glynn, G.F. Imbusch, G.P. Morgan, J. Lumin. 46 (1990) 1.
[24] M. Yamaga, B. Henderson, K.P. O'Donnell, J. Phys. Condens. Matter 1 (1989) 9175.
[25] M. Yamaga, B. Henderson, K.P. O'Donnell, C. Trager-Cowan, A. Marshall, Appl. Phys. B50 (1990) 425.
[26] B. Struve, G. Huber, Appl. Phys. B36 (1985) 195.
[27] C.J. Donnelly, T.J. Glynn, G.P. Morgan, G.F. Imbusch, J. Lumin. 48–9 (1991) 283.
[28] C.J. Donnelly, S.M. Healy, T.J. Glynn, G.F. Imbusch, G.P. Morgan, J. Lumin. 42 (1988) 119.
[29] M. Yamaga, B. Henderson, K.P. O'Donnell, G. Yue, Appl. Phys. B51 (1990) 132.
[30] M. Grinberg, P. MacFarlane, B. Henderson, K. Holliday, Phys. Rev. B52 (1995) 3917.
[31] M. Grinberg, W. Jaskólski, P.I. Macfarlane, K. Holliday, J. Phys. Condens. Matter. 9 (1997) 2815.

[32] M. Grinberg, W. Jaskòlski, P.I. McFarlane, B. Henderson, K. Holliday, J. Lumin. 72/74 (1997) 193.
[33] M. Grinberg, J. Sokólska, S. Kück, W. Jaskólski, Phys. Rev. B60 (1999) 959.
[34] I. Sokólska, S. Goląb, W. Ryba-Romanowski, Spectrochim. Acta A54 (1998) 1685.
[35] A.M. Glass, J. Chem. Phys. 50 (1969) 1501.
[36] S.T. Lai, B.H.T. Chai, M. Long, M.D. Shinn, J.A. Caird, J.E. Marion, P.R. Staver, in: A.B. Rudgor, L. Esterowitz, L.G. DeShaver (Eds.), Tunable Solid State Lasers II, Springer Verlag, Berlin, 1986, p. 145.
[37] L.J. Andrews, A. Limpicki, B.C. McCollum, C.J. Gunta, R.H. Bartram, J.F. Dolan, Phys. Rev. B34 (1986) 2735.
[38] S.A. Payne, L.L. Chase, W.F. Krupka, J. Chem. Phys. 86 (1987) 3455.
[39] L.J. Andrews, A. Lempicki, B.C. McCallum, Chem. Phys. Lett. 74 (1980) 404.
[40] H. Yersin, P. Huber, G. Gietl, D. Trümbach, Chem. Phys. Lett. 199 (1992) 1.
[41] F. Diomedi Camassei, L.S. Forster, J. Chem. Phys. 50 (1969) 2603.
[42] W. Targos, L.S. Forster, J. Chem. Phys. 44 (1966) 4342.
[43] G.F. Imbusch, T.J. Glynn, G.P. Morgan, J. Lumin. 45 (1990) 69.
[44] A. von Die, G. Blasse, W.F. van der Weg, J. Phys. C: Solid State Phys. 18 (1985) 3379.
[45] L.J. Andrews, A. Lempicki, B.C. McCollum, J. Chem. Phys. 74 (1981) 5526.
[46] M.R. Sirtlanov, J. Lumin. 59 (1994) 101.
[47] M. Haquari, M. Ajrroud, H. ben Ouada, A. Maaref, R. Brenier, C. Garapon, Phys. Status Solidi B215 (1999) 1165.
[48] M. Grinberg, K. Holliday, J. Lumin. 92 (2001) 277.
[49] F. Rasheed, K.P. O'Donnell, B. Henderson, D.B. Hollis, J. Phys. Condens. Matter 3 (1991) 3825.
[50] G.B. Porter, H.L. Schläfer, Z. Phys. Chem. (N.F.) 37 (1963) 109.
[51] H.L. Schläfer, H. Gausmann, H. Witzke, J. Chem. Phys. 46 (1967) 1423.
[52] G.E. Rojas, D. Magde, Inorg. Chem. 26 (1987) 2334.
[53] H. Yersin, H. Otto, G. Gliemann, Theor. Chim. Acta 33 (1974) 63.
[54] F. Castelli, L.S. Forster, J. Am. Chem. Soc. 97 (1975) 6306.
[55] C.D. Flint, D.J.D. Palacio, J.C.S. Faraday II 76 (1980) 82.
[56] D.M. Klassen, H.L. Schläfer, Ber. Bunsenges. Phys. Chem. 72 (1968) 663.
[57] H. Otto, H. Yersin, G. Gliemann, Z. Phys. Chem. (N.F.) 92 (1974) 193.
[58] L.S. Forster, D. Murrow, A.F. Fucaloro, Inorg. Chem. 29 (1990) 3706.
[59] K. DeArmond, L.S. Forster, Spectrochim. Acta 19 (1963) 1393.
[60] G.J. Goldsmith, F.V. Shallcross, D.S. McClure, J. Mol. Spectrosc. 16 (1965) 296.
[61] F. Diomedi Camassei, L.S. Forster, J. Mol. Spectrosc. 31 (1969) 129.
[62] L.S. Forster, J.V. Rund, F. Castelli, P. Adams, J. Phys. Chem. 88 (1982) 2395.
[63] A.D. Kirk, Chem. Rev. 99 (1999) 1607.
[64] Z. Zhang, K.T.V. Grattan, A.W. Palmer, Phys. Rev. B11 (1993) 7772.
[65] Z.Y. Zhang, K.T.V. Grattan, J. Lumin. 62 (1994) 263.